Nickel-Catalyzed Regioselective Cross-Electrophile Alkene Difunctionalization

by

Kevin Patrick Quirion

Bachelor of Science in Chemistry, Central Connecticut State University, 2018

Submitted to the Graduate Faculty of the

Dietrich School of Arts and Sciences in partial fulfillment

of the requirements for the degree of

Master of Science

University of Pittsburgh

2023

UNIVERSITY OF PITTSBURGH

DIETRICH SCHOOL OF ARTS AND SCIENCES

This thesis was presented

by

Kevin Patrick Quirion

It was defended on

September 17, 2021

and approved by

Paul Floreancig, Professor, Department of Chemistry

Yiming Wang, Assistant Professor, Department of Chemistry

Thesis Advisor: Peng Liu, Professor, Department of Chemistry

Nickel-Catalyzed Regioselective Cross-Electrophile Alkene Difunctionalization

Kevin Patrick Quirion, M.S.

University of Pittsburgh, 2023

Nickel-catalyzed alkene difunctionalization processes with two different carbon electrophiles can lead to the facile formation of many different types of C–C bonds. The use of two electrophiles with similar electronic properties is a unique application leading to regioselective bond formation utilizing commonly available and inexpensive alkyl and aryl iodides. To help explain this catalyst-controlled cross-electrophile selectivity, we utilize DFT calculations to examine the reaction mechanisms and the reactivity of aryl and alkyl iodide electrophiles in reactions with different nickel complexes. Specifically, several factors that control the reactivity of the oxidative addition with phenyl or *n*-butyl iodide are disclosed. First, the three-center cyclic oxidative addition transition states with Ni(0) complexes have a preferential reactivity with phenyl iodide in agreement with the experimental observations. The reaction of the resulting Ni(II) intermediate with the second electrophile takes place via the S_N2-type oxidative addition of *n*-butyl iodide to the 4-coordinated Ni(II) complex. The origin of the lower activation energy of the S_N2-type transition state compared to competing iodine atom transfer transition state was further examined using distortion/interaction analysis and the comparison of metal-to-electrophile charge transfer. A robust understanding for the factors promoting the cross-selectivity of aryl and alkyl iodides is important to expand the scope of the reaction and advance our understanding of nickel-catalyzed reactions.

Table of Contents

List of Tables

List of Figures

1.0 Introduction

Transition metal catalyzed alkene difunctionalizations are important tools used to add functional groups to various privileged scaffolds including biologically relevant molecules. Traditionally, it has been challenging to control regioselectivity in transition metal catalyzed multi-component reactions involving two electrophiles. Instead, these transformations are often achieved via stepwise additions; in addition to requiring careful stoichiometric control such stepwise reactions are more taxing on time and resources. As such, novel methods of alkene functionalization that may allow access to previously inaccessible compounds or otherwise expand our scope of synthetic capabilities are valuable targets for computational inquiry. The capability of utilizing two different electrophiles in a multicomponent nickel-catalyzed alkene difunctionalization (Figure 1) is a unique application of cross-electrophile catalysis, originally reported by Koh et al.[1] The electrophiles they utilized were alkyl and aryl halides, which showed

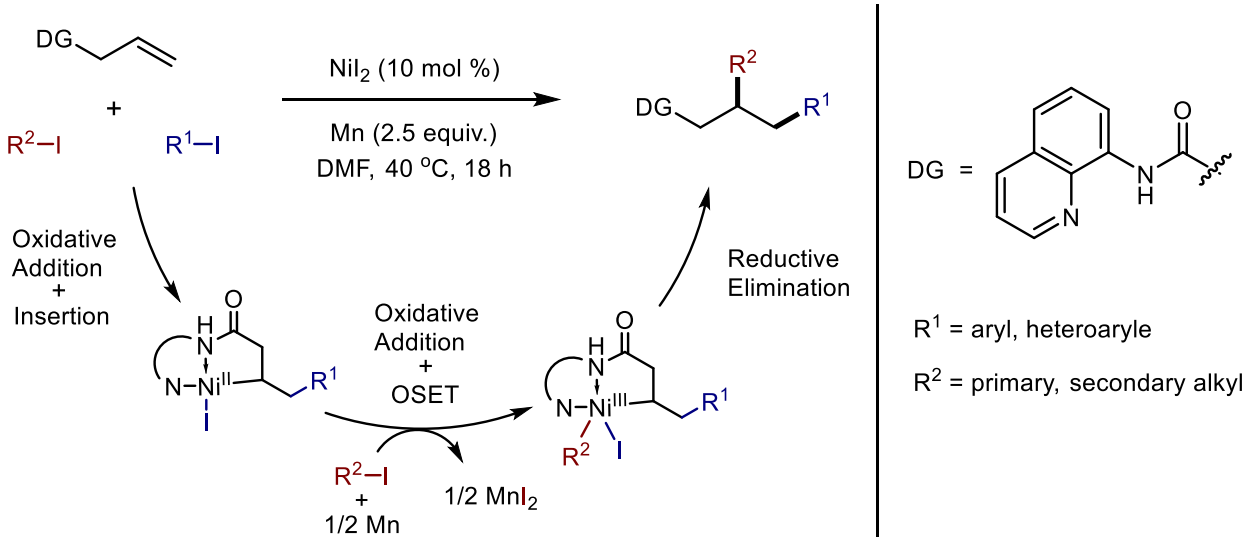

Figure 1. Ni-catalyzed regioselective alkene difunctionalization with aryl iodide and alkyl iodide electrophiles.

high levels of regioselectivity. Lin and Diao also published a cross-electrophile difunctionalization where they propose a sequential reduction mechanism with an intramolecular radical cyclization of an alkyl halide followed by functionalization with an aryl halide.[8] Despite this recent work on cross-electrophile nickel-catalyzed olefin functionalization the question of exactly how aryl and alkyl halides have different regioselectivity remains highly speculative and elucidating this mechanism is the primary focus of this paper.

1.1 Background

Another literature example of a similar alkene cross-electrophile coupling was performed by Diao and Lin; in this reaction they determined that sequential reduction was the operative mechanism. Nickel(II) was generated via reaction of the catalyst with phenyl bromide, which was then reduced by zinc to Ni(I). This Ni(I)-Ph catalyst in turn activates the alkyl bromide generating a cyclopropane radical (after rearrangement) and a Ni(II) species. After addition and reductive elimination the process affords a difunctionalized product.[8] This differs from the process we are studying in several key ways, but most importantly the alkene is lost via a Rearrangement of vinylcyclopropane to cyclopentene constituting the first site functionalized. Whereas, in the study from Koh et al. that we are investigating, the first electrophile undergoes migratory insertion generating a nickelacycle. Furthermore, single electron processes only begin to predominate around the time of the second oxidative addition in the system we are investigating; either a Ni(I) intermediate is generated by outer-sphere (OSET) just before the second oxidative addition or the OSET is undergone after the addition. However, the final steps are quite similar, where a Ni(I)

intermediate is formed after reductive elimination and the respective metal reductants regenerated the Ni(0) catalyst.

With respect to the orthogonal nature of cross-electrophile coupling, there is a minimum level of differentiation needed between the two electrophiles. Yet again, Koh et al. has done some amount of work to attempt to understand this.[7] We can see that two alkyl halide electrophiles have not been used successfully on a broad substrate scope to produce consistent orthogonal cross-electrophile couplings of alkenes. Therefore, Koh et al. pioneered a reaction system utilizing *N*-(Acyloxy)phthalimides to produce site-selective difunctionalized alkenes with two alkyl groups.[7] The phthalimide electrophiles provide a sufficient differential in reactivity to achieve this end; in the same way the alkyl and aryl halides provide sufficient differentiation for orthogonal reactivity.

Mechanisms of nickel-catalyzed alkene functionalization processes are more diverse and complex than those of palladium catalyzed processes. Nickel has been shown to proceed through both closed- and open-shell transition states and is capable of more easily accessing several possible oxidation states.[9, 21] These unique properties are mediated though nickel's tendency to favor geometries with degenerate d-orbital splitting. This tendency to form degenerate orbitals means that there is a higher probability of having unpaired electrons in singly occupied molecular orbitals (SOMOs), since this state is lower in energy than a completely empty orbital at the same energy level. Complexes containing palladium are very useful in catalysis, but their lowest unoccupied molecular orbitals (LUMOs) tend to be much higher in energy, making most open-shell species prohibitively high in energy. Furthermore, nickel will also favor oxidative addition to a greater extent than palladium owing to nickel's lower reduction potential, electronegativity and slightly smaller size. Difunctionalization is further aided by nickel species slow rate of β-

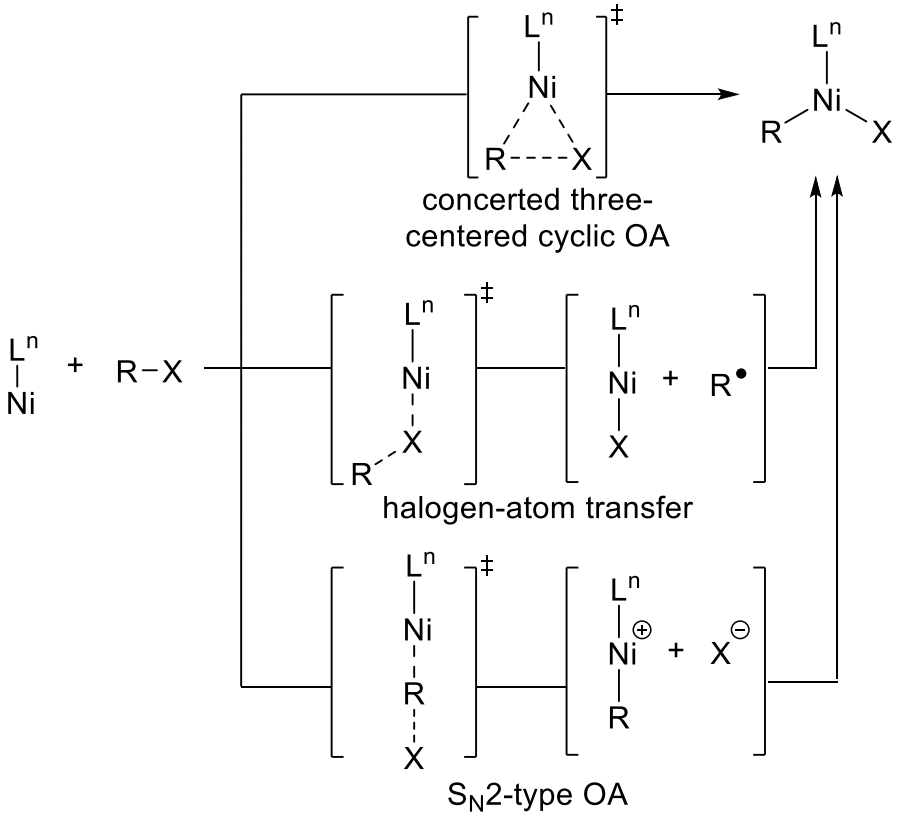

Figure 2. Several common mechanisms of oxidative addition.

hydride elimination contrasted with palladium's quick restoration of unsaturation in many systems. These properties make nickel a privileged catalyst in reactions utilizing multiple electrophiles.[9, 22]

The most common oxidative addition process found in similar systems and in general is the concerted cyclic oxidative addition process.[21, 22] This two-electron oxidative process simply breaks one bond while forming two additional bonds with the metal center. The S_N2-type oxidative addition also represents another type of two electron oxidative addition process common in these types of organometallic catalysis reactions. The third type of oxidative addition of interest in this system is the single electron inner-sphere halogen atom transfer, which results in the formation of a radical alkyl or aryl species (Figure 2). In accordance with our findings and the available literature it is documented that nickel is more amenable to a traditional three-center cyclic

oxidative addition transition state when reacting with C(sp^2) electrophiles, such as aryl halides, and more likely to proceed through an open-shell radical pathway or an S_N2-type pathway when reacting with C(sp^3) electrophiles, such as alkyl halides (Figure 2).[7-10, 22] The difference in energy between the C(sp^2) three centered cyclic process with an aryl iodide electrophile and the C(sp^3) S_N2-type oxidative addition with an alkyl iodide electrophile could help account for the observed regioselectivity in such transformations. Combined with the lack of any appreciable β-hydride elimination this explains why the nickel catalyst is a crucial component of these cross-electrophile olefin functionalizations.

These cross-electrophile functionalizations have been utilized by researchers in the areas of organic synthesis and medicinal chemistry to affect difunctionalizations.[22] Alkenes are some of the most common functional groups found in FDA approved pharmaceutical drugs and their precursors. As such, functionalizing these carbon double bonds is a common transformation in drug manufacturing and additional development of cross-electrophile couplings could even give process chemists additional options for functionalizing these compounds at scale. As previously mentioned, difunctionalizations not utilizing cross-electrophile coupling will typically utilize more labor-intensive stepwise addition. More specifically, this process typically involves at least one nucleophile, which are typically far less stable and are often required to be produced *in-situ*. Typical halogenated alkyl and aryl electrophiles are comparatively stable and are commercially available at low cost.

1.1.1 This Work

Given our previous lack of understanding regarding the precise reason for the observed difference in reactivity of aryl halide and alkyl halide electrophiles, we performed density

functional theory (DFT) calculations to understand the reaction mechanism. Computational studies comparing the relative stability of the oxidative addition transition states of the nickel complexes help to elucidate the steric and electronic causes for the orthogonal reactivity and could help future researchers design systems that are more likely to function with higher degrees of electrophile compatibility. A more complete understanding of these transition states can be further aided by analyzing the interaction energies and charge transfer between the nickel complexes and the electrophiles in the different types of oxidative addition mechanisms. Furthermore, we were interested in examining the various intermediates via DFT in order to determine the source of the orthogonal reactivity. Certain intermediates must necessarily interact differently with alkyl and aryl halides utilized by Koh et al. in order to produced the observed site selectivity. Thus we have theorized a general explanation for the experimentally determined selectivity (Figure 3) and then generated a computational model of the reaction free-energy surface using DFT (Figures 5 and 6).

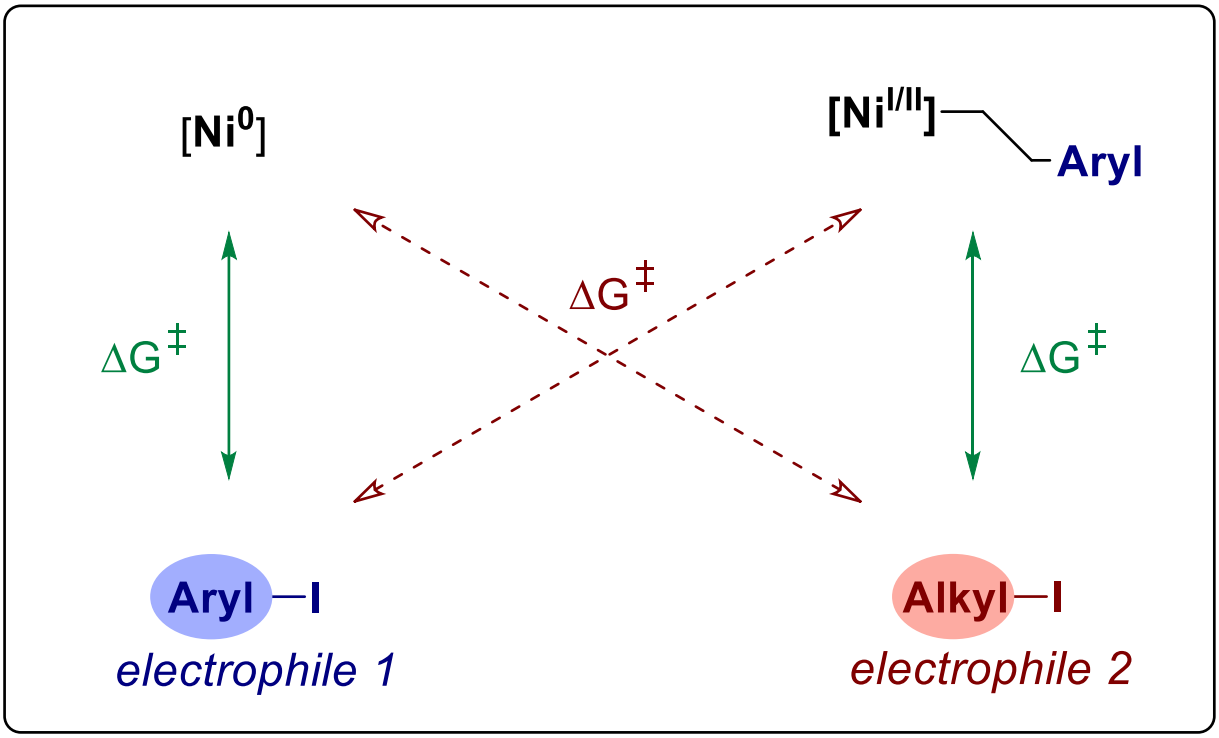

Figure 3. Hypothesized cross-electrophile selectivity with nickel intermediates.

2.0 Computational Details

All complexes shown have been optimized at the following level of theory: B3LYP-D3/SDD-6-311+G(d,p)/SMD(DMF)//B3LYP-D3/SDD-6-31G(d). All geometry optimizations were performed using the B3LYP-D3[18] functional with a mixed basis set of SDD[17] for nickel and iodine and 6-31G(d) for all other atoms. Single point energies were similarly performed using the B3LYP-D3 functional with a mixed basis set of SDD for nickel and iodine and 6-311+G(d,p) for all other atoms.[17, 18] Solvation effects were accounted for using the SMD solvation model in dimethylformamide (DMF). All density functional theory (DFT) calculations were performed using Gaussian 16 on Pitt CRC, XSEDE, and Frontera supercomputers.[20]

3.0 Results and Discussion

The proposed mechanism of the nickel-catalyzed alkene difunctionalization involves the selective oxidative addition of phenyl iodide and n-butyl iodide to two different Ni complexes in the catalytic cycle (Figure 4). This involves a Ni(0) π-complex reacting with the alkene reactant followed by a Ni(I) or Ni(II) metallacycle intermediate formed after the alkene migratory insertion. Three different types of nickel π-alkene complex, including the amide and iminol tautomers and the deprotonated complex, may be formed under the reaction conditions and involved in the reaction with the electrophile. The unique nature of this reaction is that it utilizes two similar electrophiles but retains fully orthogonal reactivity (Figure 3). Given this orthogonal reactivity, it can be reasoned that various nickel complexes along the reaction pathway have differential reactivity with phenyl iodide versus n-butyl iodide. We examined many of the nickel complex reaction intermediates and transition states using density-functional theory (DFT) to identify the key nickel complexes that control selectivity.

The proposed catalytic cycle (Figure 4) begins with a Ni(0) π-alkene complex followed by an oxidative addition with phenyl iodide and subsequent alkene migratory insertion. This is followed by an S_N2-type oxidative addition of n-butyl iodide, and subsequent reductive elimination. Other possible mechanisms involve either an outer sphere electron transfer affording Ni(I) followed by an inner sphere halogen atom transfer or a concerted three-centered cyclic oxidative addition preceding elimination. All mechanisms were then investigated using DFT calculations.

It was determined the first oxidative addition transition state (**TS1-a3**) has a higher energy than the subsequent migratory insertion transition state (**TS2a**). Therefore, the first oxidative

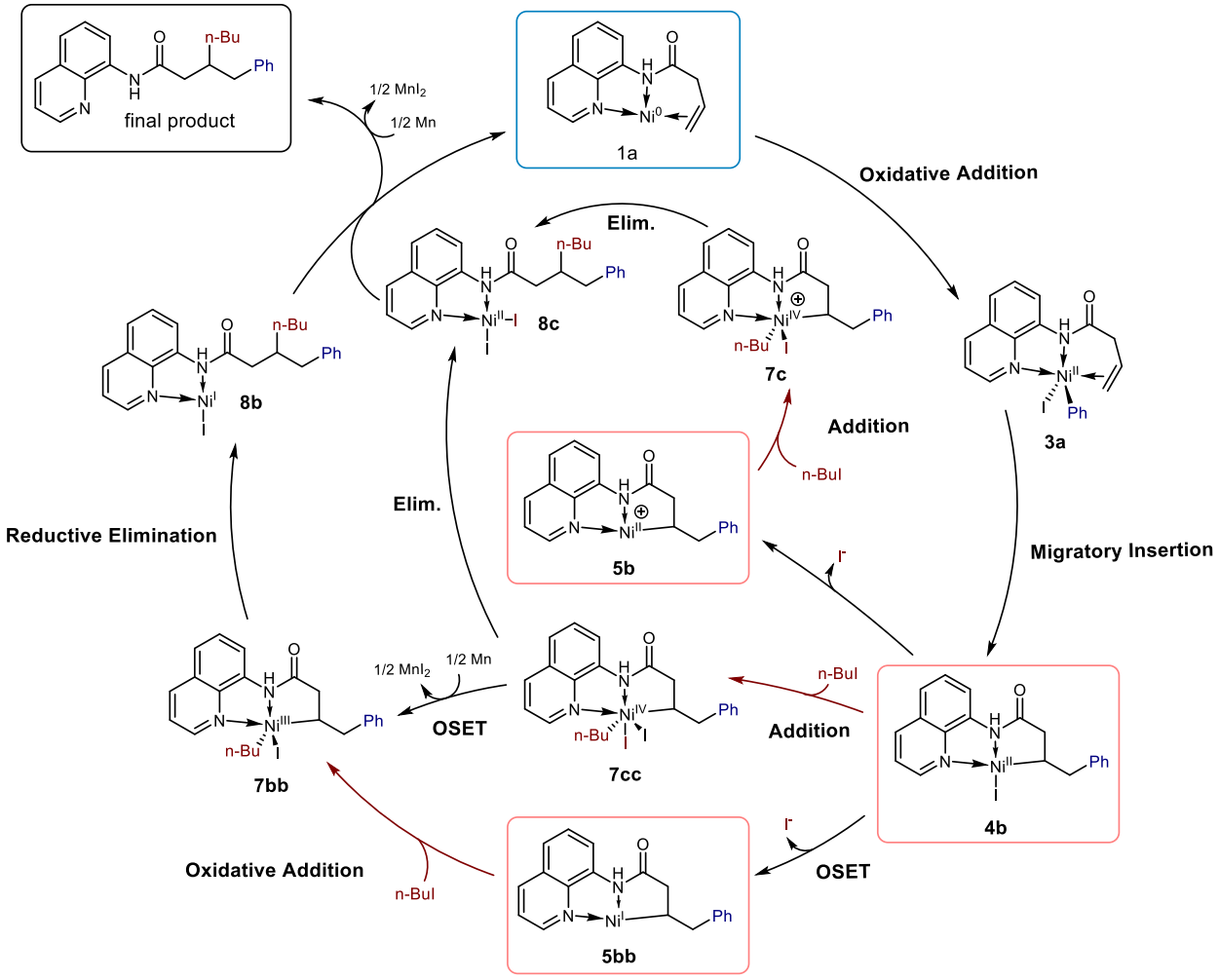

Figure 4. Proposed catalytic cycle.

addition is irreversible and controls the electrophile selectivity with the nickel(0) complex. Additionally, it was found that the complex containing the amide tautomer was the most stable tautomer form to be present until after the migratory insertion where a tautomerization is proposed; the iminol was favored in all complexes after migratory insertion (Figures 5 and 6).

The first oxidative addition was tested using both the iminol and amide tautomers, as well as the deprotonated nickel complex. The *N*,*N*-bidentate group of the starting material coordinates to Ni(0) to form the π-alkene complex (**1a**). This is followed by coordination with phenyl iodide

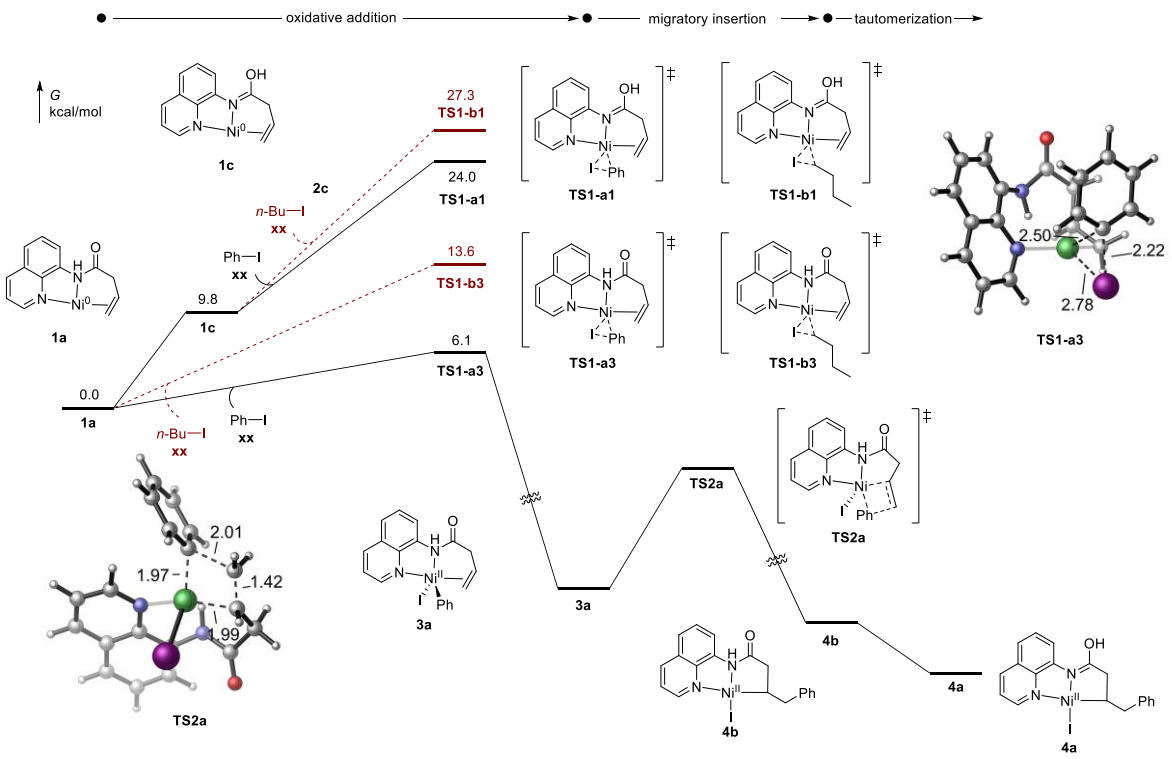

Figure 5. Reaction energy profile for the Ni(0)-Ni(II) oxidative addition and alkene migratory insertion steps.

(**2a**) and subsequent oxidative addition (**TS1-a3**). Regardless of which tautomer was reacted there was found to be a preferential reactivity with phenyl iodide over butyl iodide (Figure 5). Both iodine atom transfer and S_N2-type oxidative addition transition states have been investigated but only the S_N2-type could be located and is still higher in energy than the 3-centered cyclic transition state. All the most favorable oxidative transition states for the oxidative addition of the first electrophile have been singlet closed shell three centered cyclic transition states, which are typical for low spin Ni(0) complexs.[9, 10] In accordance with the literature on closed shell nickel oxidative additions, we observe the typical result of the aryl halide having preferential reactivity compared

to the alkyl halide. The rationale for this observed trend is that the closed shell 2-electron process favors a traditional three centered cyclic oxidative addition with C(sp^2) carbon centers over C(sp^3) carbon centers.[9] This is evidenced by the much higher distortion energy present in the butyl iodide transition state, which has similar electronic interaction energy but a 6 kcal/mol greater distortion

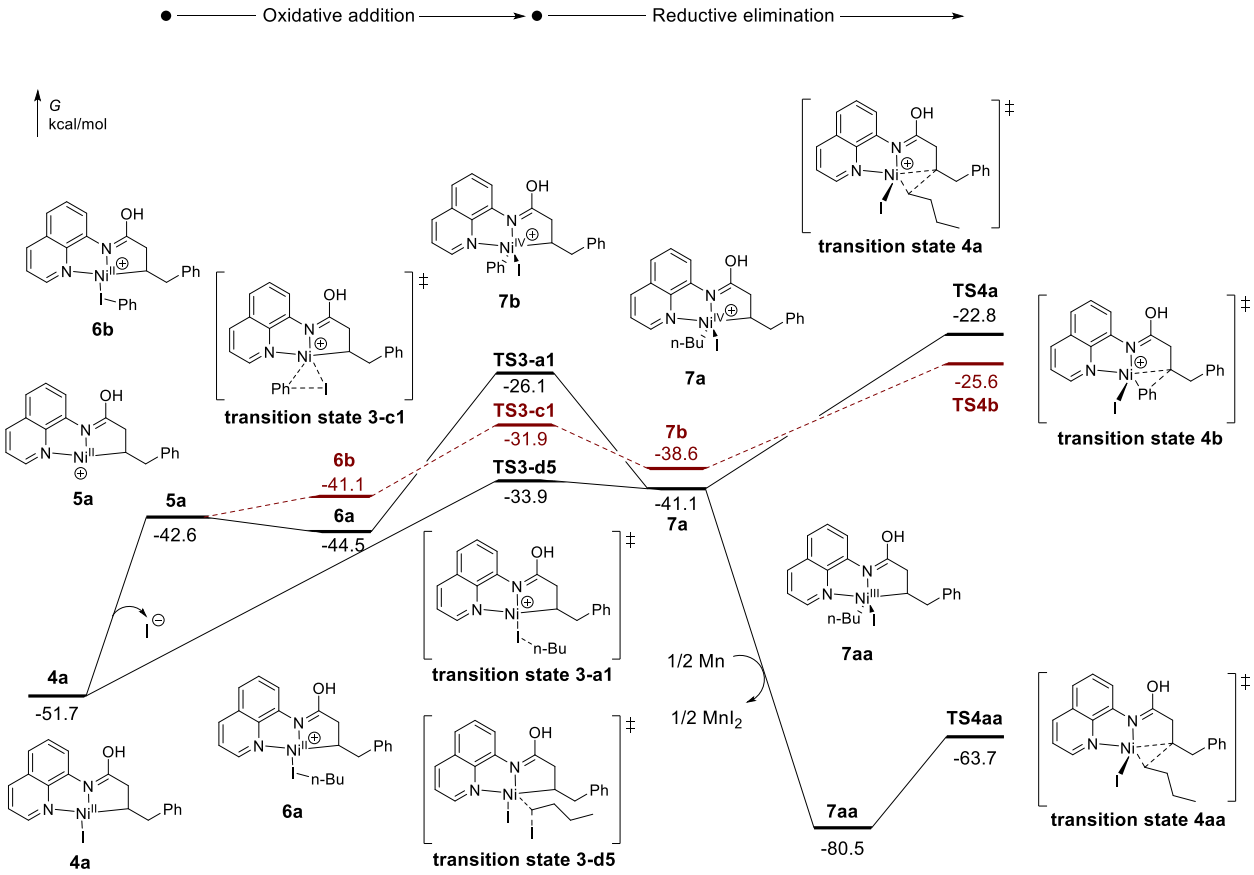

Figure 6. Reaction energy profile of possible second oxidative addition pathways involving Ni(II) metallacycle **4a**.

energy. The oxidative addition is then followed by migratory insertion of the phenyl group (TS2a), which has a significantly lower energy barrier than the oxidative addition (Figure 5). Additionally, as expected of migratory insertions between two C(sp^2) centers the phenyl group is strongly favored in the migratory insertion step over the C(sp^3) centered n-butyl group for all pathways

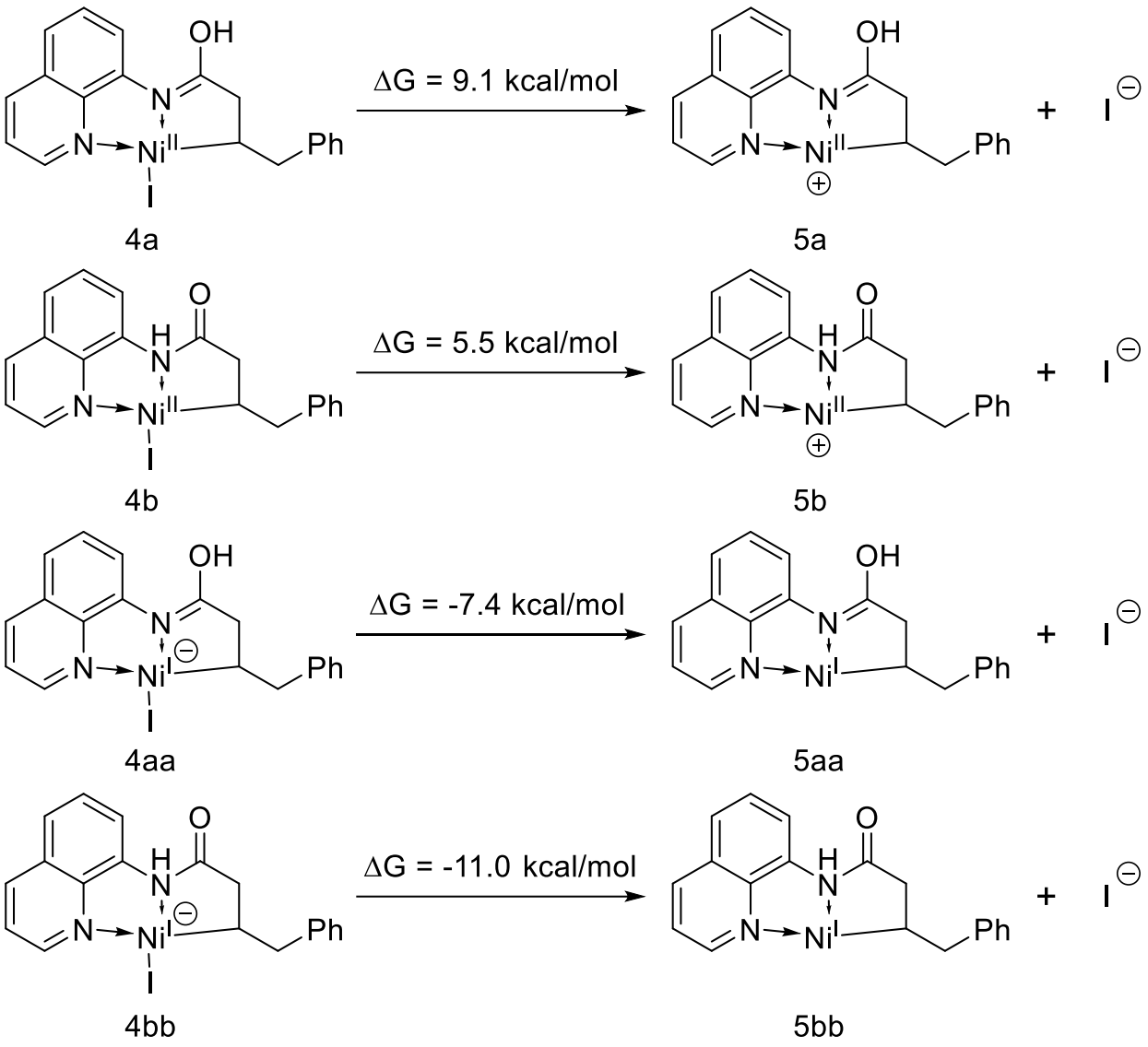

Figure 7. Gibbs free energy of iodide anion dissociation from several Ni(I) and Ni(II) complexes.

tested. This preference for oxidative addition and migratory insertion with phenyl iodide is what would be expected based on the literature.[9]

There are several plausible pathways for the reaction to proceed with after the migratory insertion (**TS2a**), formation of nickelacycle intermediate **4a**, and subsequent tautomerization to the iminol form. In the oxidative addition of the second electrophile with the nickelacycle

Table 1. Computed activation free energies of the second oxidative addition transition states with several Ni(I) and Ni(II) metallacycle intermediates.

#	intermediate	TS3-aX $\Delta G^{\ddagger}$ ($\Delta E^{\ddagger}$)	TS3-bX $\Delta G^{\ddagger}$ ($\Delta E^{\ddagger}$)	TS3-cX $\Delta G^{\ddagger}$ ($\Delta E^{\ddagger}$)	TS3-dX $\Delta G^{\ddagger}$ ($\Delta E^{\ddagger}$)
1	**4a** $\Delta G = 0.0$	28.5 (19.5)	40.5 (29.4)	**17.8** (4.6)	39.7 (27.6)
2	**4b** $\Delta G = 5.0$	30.0 (22.3)	36.5 (25.1)	25.8 (12.6)	30.9 (22.2)
3	**5bb** $\Delta G = 0.0$	10.5 (-1.3)	14.9 (1.8)	**2.5** (-8.9)	3.3 (-8.0)
4	**5aa** $\Delta G = 4.9$	7.9 (-7.1)	-- (-2.3)*	8.1 (-4.0)	9.1 (-7.2)
5	**5a** $\Delta G = 0.0$	16.5 (6.1)	14.2 (2.8)	23.8 (12.7)	**10.6** (-2.5)
6	**5b** $\Delta G = 1.4$	21.6 (11.8)	20.2 (9.2)	28.0 (17.7)	16.4 (2.9)

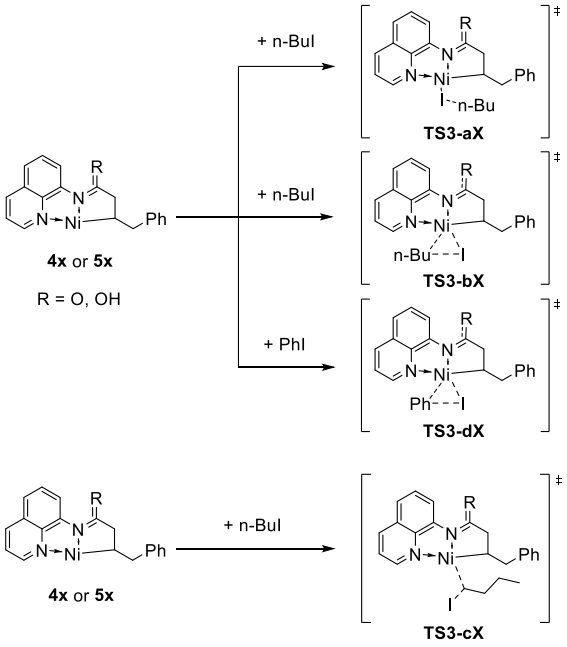

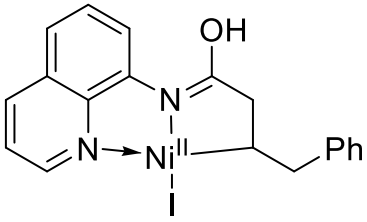

4a

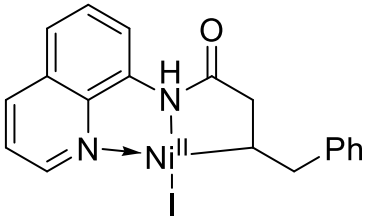

4b

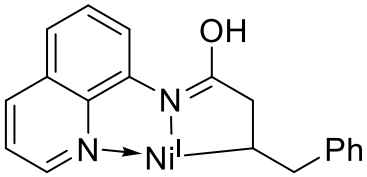

5aa

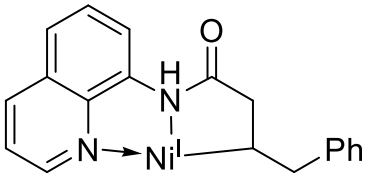

5bb

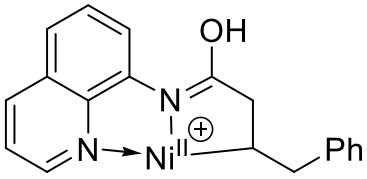

5a

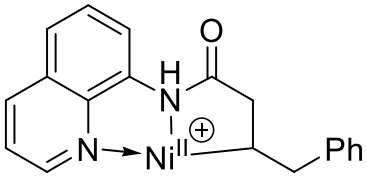

5b

intermediate **4a**, one proposed pathway begins with a single electron reduction by Mn yielding the Ni(I) nickelacycle intermediate **4aa**, which may be followed by the loss of iodide and subsequent coordination of phenyl iodide or butyl iodide (Figure 6). However, it is clear from the initial experimental paper from Koh et al. that the phenyl and butyl iodides have orthogonal reactivity, which demonstrates that the second oxidative addition step favors the reaction with butyl iodide.[1] Therefore, an open shell reaction pathway cannot be supported with any of the Ni(I) complexes located (Table 1). Similarly, the Ni(II) nickelacycle intermediate **5a** and subsequent oxidative transition state **TS3-5a** shown in Figure 6, are also energetically disfavored, probably owing to the formation of the positively charged nickelacycle upon loss of iodide (Figure 7). Alternatively, depending on which bases are present in the reaction the *O*-deprotonated complex could be present, though notably the oxidative addition of the second electrophile also shows the wrong regioselectivity for the complexes that have been located (see supporting information).

One possibility that may favor the experimentally observed selectivity is the direct S_N2-type oxidative addition to nickelacycle intermediate **4a** (**TS3-c5**), but the octahedral complex **7c** (not shown) without the loss of iodide is energetically disfavored. Alternatively, loss of iodide and formation of **7a** is also possible (Figure 6). All other complexes located point toward a more favorable reaction with phenyl iodide, which corresponds to the formation of a product not observed by Koh et al.[1] Therefore, the S_N2-type oxidative addition is believed to be the most likely pathway given the low energy barrier and lack of other options. This S_N2-type oxidative addition is the only reaction mechanism to produce the experimentally known regioselectivity. Given the high energy of TS4a we propose an outer sphere electron transfer (TS4aa), which is significantly favored at this stage of the reaction. It is worth noting that in addition to the shown profile (Figure 6) it the pathway involving intermediate 5bb also supports a viable S_N2-type pathway through

TS3-c3, though the energy difference from the competing **TS3-d3** is quite small (0.8 kcal/mol) and is less likely to account for the experimental selectivity as observed.

An in-depth screening of potential nickel complexes was examined for the second oxidative addition (Table 1) and highlights several different variables and four different types of complexes. In addition to the three centered cyclic transition states and S_N2-type complexes there were also some iodine atom transfer transition states found for butyl iodide. Some of these iodine atom transfers were found to possess a higher level of stability than their 3-centered cyclic counterparts, though they still exhibited the wrong selectivity due to the higher energy tautomers or lower energy S_N2-type oxidative additions (Table 1). Specifically, it was observed that the butyl iodide inner sphere electron transfers (ISETs) (**TS3-aX**) had a moderately lower energy than the 3-center cyclic phenyl iodide oxidative addition for entries 5, 6, 7, and 8 (Table 1). However, the S_N2-type complexes proved even more favorable for entries 1 and 3. Entries 2 and 4 were found to be higher energy tautomers, rendering favorable selectivity moot, though still instructive from an analytical standpoint. These differences in reactivity could be accounted for by the greater amenability of $C(sp^3)$ carbon centers to undergo iodine atom transfers via open shell radical pathways in typical cases, as well as the ability of $C(sp^3)$ carbon centers to undergo S_N2-type reactions.[7] It seems that the higher nucleophilicity of the Ni(I) and 4-coordinated Ni(II) intermediates is one of the factors that allows this S_N2-type reaction to occur, but it does not explain the greater relative tendency towards S_N2-type reactions for the 4-coordinated intermediates. For this we must propose a different explanation.

In the Ni(I) entries 3 and 4 the loss of iodide is spontaneous and energetically favorable, and the amide becomes the more favorable tautomer. This favorability may be due to the lower coordination number of the amide compared to the iminol for the Ni(I) complexes. Since Ni(II)

should be able to tolerate a higher coordination than Ni(I) it follows that the undistorted 3-coordinated iminol complexes have a higher stability than the amide complexes. Furthermore, though S_N2-type oxidative addition would still be favored in entry 3 the energy difference may not be sufficient to account for the experimentally observed selectivity (i.e., 0.8 kcal/mol between **TS3-d3** and **TS3-c3**). The impact of the 3-coordination of entry 3 versus the 4-coordination of entry 1 is that the relative energy of the S_N2-type transition state is significantly lower than that of the concerted mechanisms. That is, the S_N2-type transition states do not seem to incur nearly the same penalty as the concerted cyclic transitions states in reactions with 4-coordinated complexes. The most likely explanation for this phenomenon is the significant change in sterics that additional coordination imposes on this system. Since the 4-coordinated complex adopts a square planar structure there is significantly more crowding in cyclic concerted oxidative additions. Another consideration supporting this steric model is the lack of a significant difference in relative energies of S_N2-type versus concerted mechanisms across 3-coordinated intermediates regardless of charge or oxidation state. However, steric factors are not enough to account for the favorability of S_N2-type over iodine atom transfer oxidative additions in entry 1. Neither can we use this steric crowding rational to fully explain the relative favorability of the S_N2-type oxidative addition in entry 3. To account for these observations, we utilize distortion/interaction analysis and highest occupied molecular orbital (HOMO) energies.

Distortion/interaction analysis and examination of the Ni–C–I and Ni–I–C bond distances of various transition states can allow us to formulate tentative conclusions regarding the precise reason for the different regioselectivity of butyl and phenyl iodide with respect to the second oxidative addition. Examining the most favorable transition state **TS3-c1** we observe a much more favorable interaction energy than with **TS3-c5**, despite the similar Ni–C bond distance and

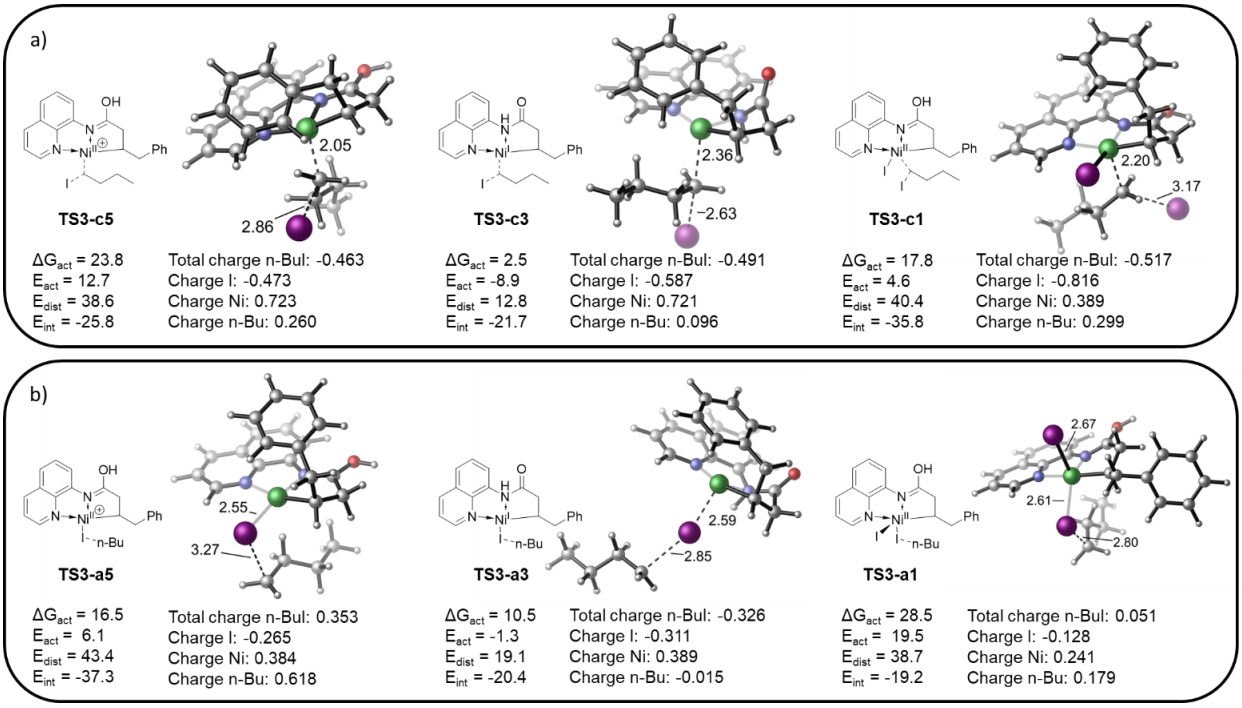

Figure 8. 3D structures of important second oxidative addition complexes, distortion/interaction energies, and corresponding NBO charge data for nickel, iodine, and n-butyl iodide. Panel a) shows the SN2-type oxidative addition transition states, and panel b) show the inner sphere iodine atom transfer transition states.

although there is a notable difference in the C–I bond distance (3.17 Å for **TS3-c1** and 2.86 Å for **TS3-c5**) the distortion energies are similar. This indicates that between the various S_N2-type oxidative addition transition states tested, the favorability is determined primarily by interaction energy and HOMO energy (Figure 8 and 9). In the case of **TS3-c5** it has a significantly greater positive charge on the nickel, a similar distortion energy, and a lower HOMO energy (Figure 8 and 9). Therefore, we can reasonably conclude it is an inferior nucleophile for the purposes of S_N2-type attacks on n-butyl iodide. Further supporting this notion is the NBO metal-to-electrophile

charge transfer, showing less negative charge transfer to the n-butyl iodide moiety in the case of **TS3-c5** compared to **TS3-c1** (Figure 8).

The reaction pathway for **TS3-c3** is slightly less viable than the pathway involing its 3-coordinated Ni(I) counterpart **TS3-c1** (Table 1). Therefore, we were able to find several similarities between the two transition states, such as: high charge transfer to the n-butyl iodide, higher interaction energy relative to distortion energy, and very high HOMO energy (Figure 8 and 9). As previously stated the energy difference between **TS3-c3** and its competing transition state **TS3-d3** is only 0.8 kcal/mol in favor of the experimentally observed selectivity.

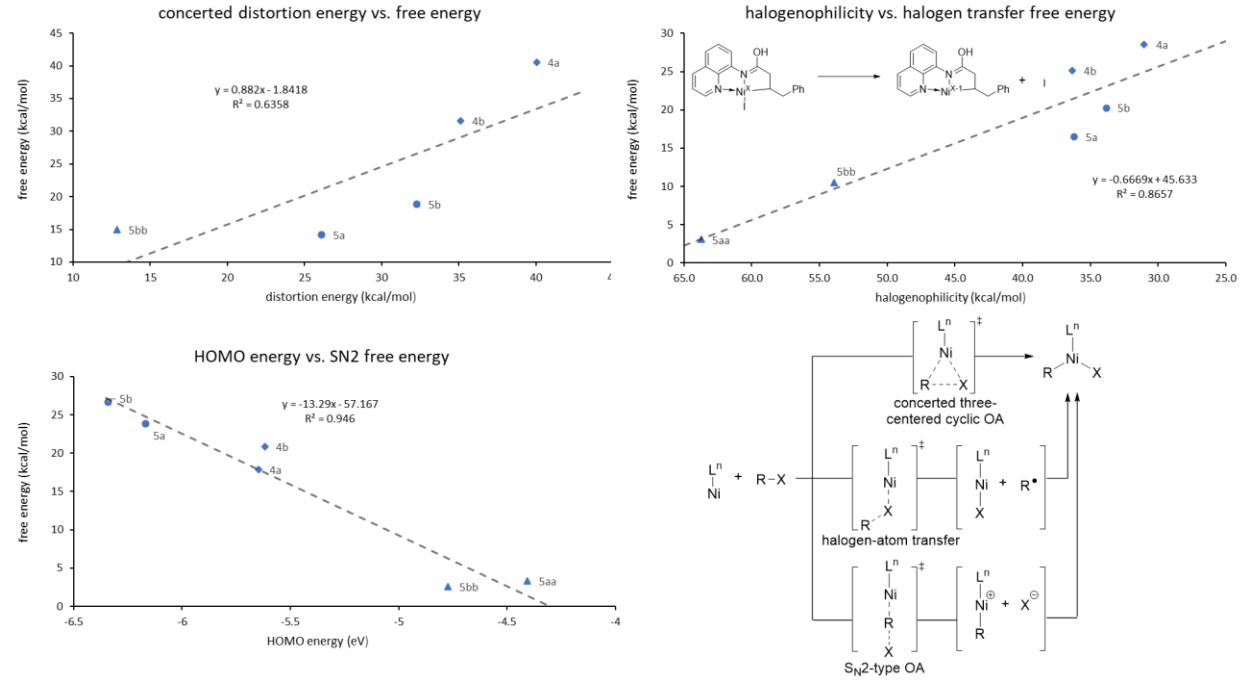

Figure 9. Graphs displaying the correlation between selectivity controlling factors and free energy for every transition state for each oxidative addition mechanism. HOMO energy versus SN2-type free energy (top left), halogenophilicity versus halogen transfer free energy (top right), distortion energy versus n-butyl iodide concerted oxidative addition free energy (bottom left), and distortion energy versus phenyl iodide concerted oxidative addition free energy (bottom right).

There is also an iodine atom transfer complex (**TS3-a1**) that shows a lower energy than its respective phenyl iodide three centered cyclic oxidative addition (**TS3-d1**). This iodine atom transfer exhibits a shorter C–I bond distance of 2.80 Å versus the 3.17 Å of **TS3-c1**, though they have similar distortion energies. Again, the stabilization from the interaction energy is significantly greater for **TS3-c1** than **TS3-a1** (Figure 8). This can probably as be explained electronically as an electron rich nickel center may be more likely to initiate an S_N2-type attack as opposed to taking on additional electron density via an iodine atom transfer.

For the halogen atom transfer oxidative addition, it seems that the halogenophilicity of the various intermediates is the primary determinant of the relative free energy of their respective transition states. We can see this evidenced by directly comparing the iodine atom transfer transition states **TS3-a1** and **TS3-a5**. The intermediate **4a** preceding **TS3-a1** has significantly lower halogenophilicity than the intermediate **5a** preceding **TS3-a5** (R^2 = 0.87, Figure 9). The positively charged **TS3-a5** only has a larger C–I bond distance of 3.27 Å due to being a later stage transition state. Furthermore, **TS3-a5** only has a modestly higher distortion energy of 43.4 kcal/mol and has a significantly more stabilizing electronic interaction energy. This is also evidenced by the higher degree of charge transfer between the iodine and n-butyl moieties in **TS3-a5** than in **TS3-a1** (Figure 8a). This is what would be expected given our previous hypotheses regarding the positively charged nickel complex, which would be expected to undergo an iodine atom transfer more easily.

In further comparing the iodine atom transfer transition states **TS3-a1** and **TS3-a3** we observe that both of these transition states are disfavored over their respective competing S_N2-type pathways. This likely has a lot to do with the relatively high HOMO energies of their respective starting intermediates (I.e. **4a** and **5bb**). In comparing these two iodine atom transfer transition

states to each other we do observe some expected differences; the 4-coordinated intermediate precursor to **TS3-a1** (**4a**) has a lower halogenophilicity than the **TS3-a3** intermediate **5bb** (Figure 8 and 9). The distortion energy of **TS3-a1** is also much higher than that of **TS3-a3**, while its charge transfer is much lower (Figure 8).

Distortion energy is nearly suffcient on its own to explain the relative energies of the phenyl iodide three centered concerted oxidative addition transition states. This is evidenced by a strong coorelation between the distortion energy and free energy of each **TS3-dX** transition state (R^2 = 0.83, See supporting information). This coorelation is noticably stonger with phenyl iodide than with butyl iodide for these three centered concerted transition states, which makes sense given the wider profile of the phenyl group. It is therefore posited that the primary factor governing the favorability of this reaction pathway is the degree to which the nickel center is serically hindered. Furthermore, interaction energy and HOMO energy have a low coorelation with the free energy of these transition states, and are therefore not considered singnificant contributors to the relative favorability of this reaction pathway (see supporting information).

3.1 Conclusions

By examining various possible reaction pathways and nickel complexes we have approached a robust understanding of the regioselectivity for this nickel catalyzed alkene difunctionalization. Given the experimental data, it is known that the final product has a powerful and exclusive regioselectivity for aryl vs alkyl iodides. The DFT calculations revealed the overall catalytic cycle involves oxidative addition of phenyl iodide to a Ni(0) π-alkene complex, followed by alkene migratory insertion, an SN2-type oxidative addition with *n*-butyl iodide, and reductive

elimination. We have formulated a robust understanding of the first oxidative addition, which favors the experimentally observed selectivity for addition with phenyl iodide (TS1-a3). We are also converging on a more complete understanding of the mechanistically complicated second oxidative addition. The most favorable reaction mechanism involves a low energy S_N2-type transition state between the 4-coordinated nickel complex and *n*-butyl iodide. Analysis of distortion/interaction energies and NBO charge transfer analysis further corroborates factors that favor the S_N2-type transition state. The interaction energy shows a more stabilizing interaction in the oxidative addition with the 4-coordinated nickel complex TS3-d5 than with a 3-coordinated nickel complex TS3-d2. The NBO charge transfer data indicates this pathway is stabilized due to a significant charge transfer to *n*-butyl iodide, consistent with the strong interaction energy with the Ni complex.

Appendix A Terminology and Acronyms

DFT - density functional theory

ISET - inner-sphere electron transfer

NBO - natural bond orbital

OSET - outer-sphere electron transfer

SMD - solvation model based on density

References

1. Yang, T.; Chen, X.; Rao, W.; Koh, M. J. Broadly Applicable Directed Catalytic Reductive Difunctionalization of Alkenyl Carbonyl Compounds. *Chem.*, **2019**, *6* (3), pp 738–751.

2. Zhang, J. S.; Liu, L.; Chen, T.; Han, L. B. Transition-Metal-Catalyzed Three-Component Difunctionalizations of Alkenes. *Chem. Asian J.*, **2018**, *13* (7), pp 2277–2291.

3. Gao, P.; Chen, L.; Brown M. K. Nickel-Catalyzed Stereoselective Diarylation of Alkenylarenes. *J. Am. Chem. Soc*. **2018**, *140* (34), pp 10653–10657.

4. Qi, X.; Wang, J.; Dong, Z.; Dong, G.; Liu, P. Compatibility Score for Rational Electrophile Selection in Pd/NBE Cooperative Catalysis. *Chem.*, **2020**, *6* (10), pp 2810–2825.

5. Sanford, A. B.; Thane, T. A.; McGinnis T. M.; Chen, P.; Hong, X.; Jarvo, E. R. Nickel-Catalyzed Alkyl–Alkyl Cross-Electrophile Coupling Reaction of 1,3-Dimesylates for the Synthesis of Alkylcyclopropanes. *J. Am. Chem. Soc.*, **2020**, *142*, pp 5017–5023.

6. Omer, H. M.; Liu, P. Computational Study of the Ni-Catalyzed C–H Oxidative Cycloaddition of Aromatic Amides with Alkynes. *ACS Omega*, **2019**, *4*, pp 5209–5220.

7. Yang, T.; Jiang, Y.; Luo, Y.; Lim, J. J. H.; Lan, Y.; Koh, M. J. Chemoselective Union of Olefins, Organohalides, and Redox-Active Esters Enables Regioselective Alkene Dialkylation. *J. Am. Chem. Soc.*, **2020**, *142* (51), pp 21410–21419.

8. Lin, Q.; Diao, T. Mechanism of Ni-Catalyzed Reductive 1,2-Dicarbofunctionalization of Alkenes. *J. Am. Chem. Soc.*, **2019**, *141* (44), pp 17937–17948.

9. Diccianni, J.; Lin, Q.; Diao, T. Mechanisms of Nickel-Catalyzed Coupling Reactions and Applications in Alkene Functionalization. *Acc. Chem. Res.*, **2020**, *53* (4), 906–919.

10. Kehoe, R.; Mahadevan, M.; Manzoor, A.; McMurray, G.; Wienefeld, P.; Baird, M. C.; Budzelaar, P. H. M. Reactions of the Ni(0) Compound $Ni(PPh_3)_4$ with Unactivated Alkyl Halides: Oxidative Addition Reactions Involving Radical Processes and Nickel(I) Intermediates. *Organometallics*, **2018**, *37* (15), pp 2450–2467.

11. Lin, X.; Phillips, D. L. Density Functional Theory Studies of Negishi Alkyl–Alkyl Cross-Coupling Reactions Catalyzed by a Methylterpyridyl-Ni(I) Complex. *J. Org. Chem.*, **2008**, *73*, 3680–3688.

12. Yoo, C.; Ajitha, M. J.; Jung, Y.; Lee, Y. Mechanistic Study on C–C Bond Formation of a Nickel(I) Monocarbonyl Species with Alkyl Iodides: Experimental and Computational Investigations. *Organometallics*, **2015**, *34*, 4305–4311.

13. Lin, X.; Sun, J.; Xi, Y.; Lin, D. How Racemic Secondary Alkyl Electrophiles Proceed to Enantioselective Products in Negishi Cross-Coupling Reactions. *Organometallics*, **2011**, *30*, 3284–3292.

14. (a) Wang, X.; Ma, G.; Peng, Y.; Pitsch, C. E.; Moll, B. J.; Ly, T. D.; Wang, X.; Gong, H. Ni-Catalyzed Reductive Coupling of Electron-Rich Aryl Iodides with Tertiary Alkyl Halides *J. Am. Chem. Soc.*, **2018**, *140*, 14490−14497. (b) Sardini, S. R.; Lambright, A. L.; Trammel, G. L.; Omer, H. M.; Liu, P.; Brown, M. K. Ni-Catalyzed Arylboration of Unactivated Alkenes: Scope and Mechanistic Studies *J. Am. Chem. Soc.*, **2019**, *141*, 9391−9400.

15. Hosseini, F. N.; Ariafard, A.; Rashidi, M.; Azimi, G.; Nabavizadeh, S. M. Density functional studies of influences of Ni triad metals and solvents on oxidative addition of MeI to $[M(CH_3)_2(NH_3)_2]$ complexes and C–C reductive elimination from $[M(CH_3)_3(NH_3)_2I]$ complexes *J. Organomet. Chem.*, **2011**, *696*, 3351–3358.
16. Xu, S.; Hirano, K.; Miura, M. Nickel-Catalyzed Regio- and Stereospecific C–H Coupling of Benzamides with Aziridines. *Org. Lett.*, **2021**, *23*, 5471–5475.
17. Andrae, D.; Haeussermann, U.; Dolg, M.; Stoll, H.; Preuss, H. Energy-adjusted ab initio pseudopotentials for the second and third row transition elements. *Theor. Chem. Acc.*, **1990**, 77, 123−141.
18. (a) Lee, C.; Yang, W.; Parr, R. G. Development of the ColleSalvetti correlation-energy formula into a functional of the electron density. *Phys. Rev. B: Condens. Matter Mater. Phys.* **1988**, *37*, 785−789. (b) Becke, A. D. Density-functional thermochemistry. III. The role of exact exchange. *J. Chem. Phys.* **1993**, *98*, 5648−5652. (c) Grimme, S. Semiempirical GGA-type density functional constructed with a long-range dispersion correction. *J. Comput. Chem.*, **2006**, *27*, 1787−179.
19. Kim, S.; Goldfogel, M. J.; Gilbert, M. M.; Weix, D. J. Nickel-Catalyzed Cross-Electrophile Coupling of Aryl Chlorides with Primary Alkyl Chlorides. *J. Am. Chem. Soc.*, **2020**, *142* (22), 9902-9907.
20. Frisch, M. J.; Trucks, G. W.; Schlegel, H. B.; Scuseria, G. E.; Robb, M. A.; Cheeseman, J. R.; Scalmani, G.; Barone, V.; Petersson, G. A.; Nakatsuji, H.; Li, X.; Caricato, M.; Marenich, A. V.; Bloino, J.; Janesko, B. G.; Gomperts, R.; Mennucci, B.; Hratchian, H. P.; Ortiz, J. V.; Izmaylov, A. F.; Sonnenberg, J. L.; Williams-Young, D.; Ding, F.; Lipparini, F.; Egidi, F.; Goings, J.; Peng, B.; Petrone, A.; Henderson, T.; Ranasinghe, D.; Zakrzewski,

V. G.; Gao, J.; Rega, N.; Zheng, G.; Liang, W.; Hada, M.; Ehara, M.; Toyota, K.; Fukuda, R.; Hasegawa, J.; Ishida, M.; Nakajima, T.; Honda, Y.; Kitao, O.; Nakai, H.; Vreven, T.; Throssell, K.; Montgomery, J. A., Jr.; Peralta, J. E.; Ogliaro, F.; Bearpark, M. J.; Heyd, J. J.; Brothers, E. N.; Kudin, K. N.; Staroverov, V. N.; Keith, T. A.; Kobayashi, R.; Normand, J.; Raghavachari, K.; Rendell, A. P.; Burant, J. C.; Iyengar, S. S.; Tomasi, J.; Cossi, M.; Millam, J. M.; Klene, M.; Adamo, C.; Cammi, R.; Ochterski, J. W.; Martin, R. L.; Morokuma, K.; Farkas, O.; Foresman, J. B.; Fox, D. J., *Gaussian 16*, revision C.01; Gaussian, Inc., Wallingford CT, 2016.

21. Hartwig, J. F. Oxidative Addition of Polar Reagents. In *Organotransition metal chemistry: from bonding to catalysis*; University Science Books: Sausalito, **2010**, pp. 301–317.
22. Duan, A.; Xiao, F.; Lan, Y.; Niu, L. Mechanistic views and computational studies on transition-metal-catalyzed reductive coupling reactions. *Chem. Soc. Rev.*, **2022**, *51*, 9986.